DEVELOPMENT OF A FLUID-SOLID MULTIPHASE FLOW SIMULATOR BY A SPH-DEM COUPLED METHOD FOR SIMULATING A SEAWALL DESTRUCTION DUE TO SOIL FOUNDATION SCOUR

KENSUKE HARASAKI [1] AND MITSUTERU ASAI [2]

[1] Department of Civil Engineering, Graduate School of Engineering, Kyushu University
Motoka744, Nishi-ku, Fukuoka 819-0395, JAPAN
e-mail: harasaki@doc.kyushu-u.ac.jp,
web page: https://kyushu-u.wixsite.com/structural-analysis

[2] Ph.D., Associate Prof., Department of Civil Engineering, Graduate School of Engineering, Kyushu University
Motoka744, Nishi-ku, Fukuoka 819-0395, JAPAN
e-mail: asai@doc.kyushu-u.ac.jp,
web page: https://kyushu-u.wixsite.com/structural-analysis

Key words: Scouring, Seepage flow, Breakwater, SPH-DEM coupled method.

Abstract. In 2011, Tohoku-Kanto earthquake tsunami caused serious damage to the port and coastal structures such as breakwaters and seawalls. The damage mechanism of these structures has been studied in the past, and it is found that there are some causes. In this study, a new simulation tool taking account of the soil scouring and seepage flow phenomena is developed to represent and predict the collapse of the breakwater with SPH-DEM coupled method.

1 INTRODUCTION

In 2011, the huge tsunami induced by the Tohoku-Kanto earthquake caused very serious damages to the port structures, especially the coastal breakwaters. Damage mechanism of the breakwater has been studied in the past, and there are three main causes; (I) horizontal force due to the water level difference between the front and rear part of breakwater, (II) soil scouring behind the breakwater during overflow and (III) piping destruction associated with the decline of the soil durability by seepage flow. Fluid-Structure-Soil coupling simulation is desired for a systematic comprehension of the breakwater collapse mechanism as it may help to develop the next disaster prevention guidelines.

In our previous study, the analysis of free surface and seepage flow related to the third cause, (III) piping destruction, is conducted with the stabilized ISPH method proposed by M. Asai et al. [1]. However, this analysis is limited to the prediction of the breakwater destruction because the mound soil was not modelled. The modelling of the soil motion is needed to analyze the break water destruction and also the second cause, (II) soil scouring. In the scouring domain, water and soil are moving each other, thus the flow comes to be a multiphase flow.

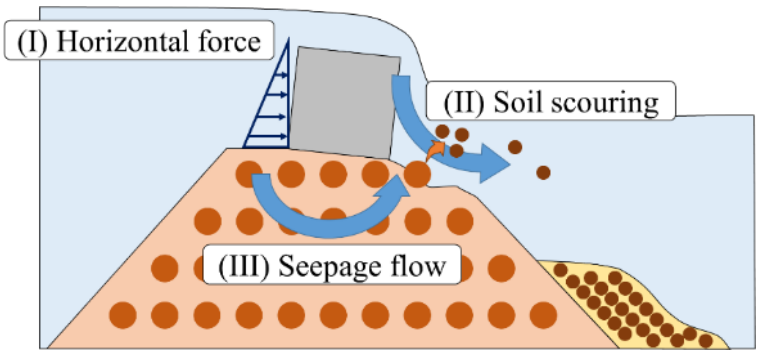

Figure 1: Main factors of the breakwater collapse

In this study, in addition to ISPH method for fluid analysis, Discrete Element Method (DEM) is selected to analyze the mound soil motion. In addition, this coupled method considering soil scouring and seepage flow is applied to the simple breakwater destruction analysis.

2 SPH-DEM COUPLING MODEL

A coupling model of ISPH method and DEM is the core in the multiphase flow analysis, and there are two models to couple ISPH method and DEM. One is the “Direct pressure model” we call. In general, a solid in fluid moves by receiving a pressure from fluid. In this method, a solid also moves in same way. However, if this method is adopted, the diameter of fluid particles need to be much smaller than the solid to calculate a force acting on the solid surface accurately. Therefore, the analysis cost is high to analyze a large scale model such as a breakwater collapse with this method. The other method is “Interaction force model”. In this method, a fluid particle can overlap with solid particles, and a fluid pressure don’t acts on a solid particle. Instead of a pressure, an interaction force acts on each particles, a resistance force on fluid and a drag force on solid. Furthermore, the diameter of fluid particle can be almost the same size with a solid

particle. This method can reduce the analysis cost compared than “Direct pressure model”, therefore “Interaction force model” is adopted to analyze.

3 ANALYSIS MEHOD

3.1 The unified governing equation

In the breakwater collapse analysis, a fluid flow will be regarded as a free surface flow in a fluid domain and a seepage flow in a mound. According to Akbari, H. [2], an unified governing equation for modelling both surface and seepage flows can be written as:

$$\frac{C_r(\varepsilon)}{\varepsilon}\frac{D\overline{\boldsymbol{v}}_f}{Dt} = -\frac{1}{\rho_f}\nabla P + \boldsymbol{g} + \nu_E(\varepsilon)\nabla^2\overline{\boldsymbol{v}}_f - a(\varepsilon)\overline{\boldsymbol{v}}_f - b(\varepsilon)\overline{\boldsymbol{v}}_f\left|\overline{\boldsymbol{v}}_f\right|, \tag{1}$$

$$\frac{D\bar{\rho}_f}{Dt} + \bar{\rho}_f\nabla\cdot\left(\frac{\overline{\boldsymbol{v}}_f}{\varepsilon}\right) = 0, \tag{2}$$

where ρ_f, $\boldsymbol{g}$, P and ε represent the original fluid density, the gravitational acceleration, the fluid pressure and the porosity. $\overline{\boldsymbol{v}}_f$ is the Darcy velocity which is understood as a spatially averaged velocity given by $\overline{\boldsymbol{v}}_f = \varepsilon\boldsymbol{v}_f$, $\boldsymbol{v}_f$ is the intrinsic fluid velocity. Here, $\bar{\rho}_f$ denotes the apparent density, which is given by $\bar{\rho}_f = \varepsilon\rho_f$. This relation regarding the apparent density is necessary to be employed in order to satisfy the volume conservation of fluid inside the porous medium. Some of the coefficient are defined as:

$$C_r(\varepsilon) = 1 + 0.34\frac{1-\varepsilon}{\varepsilon}, \tag{3}$$

$$\nu_E(\varepsilon) = \frac{\nu_w+\nu_T}{\varepsilon}, \tag{4}$$

$$a(\varepsilon) = \alpha_c\frac{\nu_w(1-\varepsilon)^2}{\varepsilon^3{d_s}^2}, \tag{5}$$

$$b(\varepsilon) = \beta_c\frac{(1-\varepsilon)}{\varepsilon^3 d_s}, \tag{6}$$

where $C_r(\varepsilon)$ is the inertial coefficient to evaluate the additional resistance force caused by the virtual mass, while $\nu_E(\varepsilon)$ is the effective viscosity including the kinematic viscosity of the fluid ν_w and the turbulent viscosity ν_T. The Smagorinsky model is adopted to define the eddy viscosity. $a(\varepsilon)$ and $b(\varepsilon)$ are the linear and non-linear coefficients, α_c and β_c in these equation are defined as the constant in our analysis. Moreover, d_s is the diameter of a solid particle. Here, the fourth and fifth terms in right side of Eq. (1) means the resistance force from the porous medium. This unified governing equation is proposed by Akbari to represent the seepage flow in a fixed porous medium with a low porosity. However, in the scouring domain, the soil as a porosity medium also moves and the porosity comes to be high. Therefore, the resistance force terms in Eq. (1) are modified referring to Wen and Yu [3], and the unified governing equation is rewritten as:

$$\frac{C_r(\varepsilon)}{\varepsilon}\frac{D\overline{\boldsymbol{v}}_f}{Dt} = -\frac{1}{\rho_f}\nabla P + \boldsymbol{g} + \nu_E(\varepsilon)\nabla^2\overline{\boldsymbol{v}}_f \begin{cases} -a(\varepsilon)\varepsilon\boldsymbol{v}_r - b(\varepsilon)\varepsilon^2\boldsymbol{v}_r|\boldsymbol{v}_r| & (\varepsilon < 0.8) \\ -\frac{3}{4}C_d\frac{(1-\varepsilon)\rho_f\boldsymbol{v}_r|\boldsymbol{v}_r|}{d_s}\varepsilon^{-2.7} & (\varepsilon \geq 0.8) \end{cases}. \tag{7}$$

Here, in considering the movement of the porous medium, the velocity in resistance force terms is changed to relative velocity $\boldsymbol{v}_r$ between fluid and solid which is given by $\boldsymbol{v}_r = \boldsymbol{v}_f - \boldsymbol{v}_s$. In taking a relative velocity, the fluid velocity must not be a spatially averaged velocity $\overline{\boldsymbol{v}}_f$ but an original velocity $\boldsymbol{v}_f$. Thus, the porosity ε is multiplied by the linear and non-linear coefficients.

In addition, the resistance force proposed by Wen and Yu for the high porosity domain ($\varepsilon \geq 0.8$) is considered. C_d is drag coefficient and defined with Reynolds number R_e as follows:

$$C_d = \frac{24\{1+0.15*{R_e}^{0.687}\}}{R_e} \qquad (R_e < 1000), \tag{8}$$

$$C_d = 0.43 \qquad (R_e > 1000), \tag{9}$$

$$R_e = \frac{\varepsilon \rho_f d_s |\boldsymbol{v}_f - \boldsymbol{v}_s|}{\nu_w}. \tag{10}$$

According to Eq. (7), the fluid flow outside the porous medium can be given by the Navier-Stokes equation with the porosity $\varepsilon = 1$. On the other hand, the fluid flow inside the porous medium can be described by including the resistance force. Eq. (2) represents the unified continuity equation for a compressible fluid.

The resistance force in Eq. (1) acts on fluid as a resistance force, and it needs to act on the porous medium as a drag force in the opposite sign as well to satisfy the action-reaction law. Thus, this resistance force can be considered as the interaction force between fluid and solid. The drag force as the interaction force for solid is described later.

3.2 The SPH method

In this study, the incompressible smoothed particle hydrodynamics (ISPH) method is adopted to solve the unified governing equation. The basic concept in SPH method is that for any function ϕ attached to particle "i" located at $\boldsymbol{x}_i$ is represented by the following volume summation:

$$\phi(\boldsymbol{x}_i) \approx \langle \phi_i \rangle := \sum_j \frac{m_j}{\rho_j} \phi_j W(r_{ij}, h), \tag{11}$$

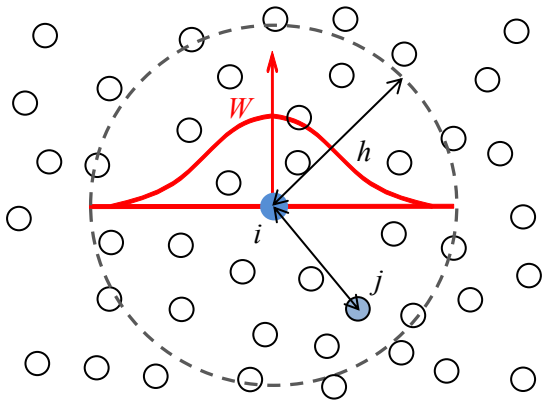

Figure 2: Particle placement and influence radius in the SPH method

where m and W are the representative volume of particle and a weight function known as the smoothing kernel function. j is a particle in the smoothing length h and r_{ij} is the length of the relative coordinate vector $\boldsymbol{r}_{ij}(= \boldsymbol{x}_j - \boldsymbol{x}_i)$. In this study, the smoothing length set to 2.4 times the initial diameter of the particle. The divergence $\nabla \cdot \phi$, the gradient $\nabla \phi$ and the Laplacian $\nabla^2 \phi$ can be written as:

$$\nabla \cdot \phi(\boldsymbol{x}_i) \approx \langle \nabla \cdot \phi_i \rangle = \frac{1}{\rho_i} \sum_j m_j (\phi_j - \phi_i) \cdot \nabla W(r_{ij}, h), \tag{12}$$

$$= \rho_i \sum_j m_j \left(\frac{\phi_j}{{\rho_j}^2} + \frac{\phi_i}{{\rho_i}^2} \right) \cdot \nabla W(r_{ij}, h), \tag{13}$$

$$\nabla \phi(\boldsymbol{x}_i) \approx \langle \nabla \phi_i \rangle = \frac{1}{\rho_i} \sum_j m_j (\phi_j - \phi_i) \nabla W(r_{ij}, h), \tag{14}$$

$$= \rho_i \sum_j m_j \left(\frac{\phi_j}{{\rho_j}^2} + \frac{\phi_i}{{\rho_i}^2} \right) \nabla W(r_{ij}, h), \tag{15}$$

$$\nabla^2 \phi(\boldsymbol{x}_i) \approx \langle \nabla^2 \phi_i \rangle = \sum_j m_j \left(\frac{\rho_i + \rho_j}{\rho_i \rho_j} \frac{\boldsymbol{r}_{ij} \cdot \nabla W(r_{ij}, h)}{{\boldsymbol{r}_{ij}}^2 + \eta^2} \right) (\phi_i - \phi_j). \tag{16}$$

Note that the triangle bracket $\langle \cdot \rangle$ indicates the SPH approximation of a particular function. η is the parameter to avoid division by zero and defined by the following expression $\eta^2 = 0.0001(h/2)^2$.

3.3 Formulation of the unified governing equation in the stabilized ISPH method

In ISPH method, the governing equation is discretized in time by the projection method based on the predictor and corrector scheme. In this method, the pressure is calculated implicitly and the velocity fields are updated explicitly. The unified governing equations, Eq. (2) and Eq. (7), are discretized as same way.

To begin with the discretization, $\overline{\boldsymbol{v}}_f$ at $n+1$ step is written as:

$$\overline{\boldsymbol{v}}_f^{n+1} = \overline{\boldsymbol{v}}_f^* + \Delta \overline{\boldsymbol{v}}_f^*, \tag{17}$$

where $\overline{\boldsymbol{v}}_f^*$ and $\Delta \overline{\boldsymbol{v}}_f^*$ are the predictor term and the corrector them respectively. Based on the projection method. Eq. (7) can be separated as:

$$\overline{\boldsymbol{v}}_f^* = \overline{\boldsymbol{v}}_f^n + \frac{\varepsilon \Delta t}{C_r(\varepsilon)} \left(\boldsymbol{g} + \nu_E(\varepsilon) \nabla^2 \overline{\boldsymbol{v}}_f^n - \boldsymbol{\gamma}^n \right), \tag{18}$$

$$\Delta \overline{\boldsymbol{v}}_f^* = \frac{\varepsilon \Delta t}{C_r(\varepsilon)} \left(-\frac{1}{\rho_f} \nabla P^{n+1} \right), \tag{19}$$

where $\boldsymbol{\gamma}$ summatizes the resistance terms in Eq. (7) as follows:

$$\boldsymbol{\gamma}^n = \begin{cases} -a(\varepsilon) \varepsilon \boldsymbol{v}_r^n - b(\varepsilon) \varepsilon^2 \boldsymbol{v}_r^n |\boldsymbol{v}_r^n| & (\varepsilon < 0.8) \\ -\frac{3}{4} C_d \frac{(1-\varepsilon) \rho_f \boldsymbol{v}_r^n |\boldsymbol{v}_r^n|}{d_s} \varepsilon^{-2.7} & (\varepsilon \geq 0.8) \end{cases}. \tag{20}$$

The pressure P^{n+1} in Eq. (19) is determined by the Pressure Poisson Equation as follows:

$$\nabla^2 P^{n+1} = \frac{C_r(\varepsilon) \rho_f}{\varepsilon \Delta t} \nabla \cdot \overline{\boldsymbol{v}}_f^*. \tag{21}$$

These equation are calculated with the concept of ISPH method. The position of a particle is updated at the end of each time step.

However, the particle density may change slightly from the initial value because the numerical particle density is calculated from the distribution of particles in the particle method. To avoid this change, the relaxation term is added to the original Pressure Poisson Equation in the stabilized ISPH method proposed by M. Asai et al.. With this concept, the Pressure Poisson Equation (Eq. (21)) is modified as follows:

$$\langle \nabla^2 P^{n+1} \rangle \approx \frac{C_r(\varepsilon)}{\varepsilon} \left(\frac{\rho_f}{\Delta t} \langle \nabla \cdot \vec{\boldsymbol{v}}_f^* \rangle + \alpha \frac{\bar{\rho}_f^n - \langle \bar{\rho}_f^n \rangle}{\Delta t^2} \right), \tag{22}$$

where α is called as the relaxation coefficient and is generally set to be much less than 1. In this study, α is set to 0.01. The analysis with the stabilized ISPH method can get good conservation of volume.

3.4 The equation of motion of soil in fluid

In this study, the soil motion is analyzed by a spherical Discrete Element Method (DEM). In general, the contact detection is done every time step and a DEM particle moves by receiving the contact forces in DEM. In addition to that, the fluid force also acts on the DEM particles in the fluid domain. There some kinds of the fluid forces, however the all of them don't influence the particle's motion. In this study, the buoyancy force and drag force are adopted to the fluid forces, the equation of motion of soil in fluid is written as follows with the contact force:

$$m_s \frac{d\boldsymbol{v}_s}{dt} = m_s \boldsymbol{g} - \nabla P V_s + \boldsymbol{F}_d + \sum \boldsymbol{F}_c, \tag{23}$$

where m_s, $\boldsymbol{v}_s$ and V_s are the mass, the velocity and the volume of a soil particle respectively. The second and third terms in right side are the fluid forces, the second is the buoyancy force and the third $\boldsymbol{F}_d$ is the drag force. $\boldsymbol{F}_c$ means the contact force between DEM particles. The equation of angular motion for the spherical DEM is given by:

$$I \frac{d\boldsymbol{\omega}}{dt} = \sum \boldsymbol{T}, \tag{24}$$

where $\boldsymbol{\omega}$ and $\boldsymbol{T}$ are the angular velocity and torque of contact forces. I is the moment of inertia and given as a constant value for a sphere.

The contact force between the particles or particle-wall is calculated by the intrusion of a particle with a spring-dashpot model in DEM. The contact force $\boldsymbol{F}_c$ is divided into two components, a repulsive force in the normal direction $\boldsymbol{F}_c^n$ and a friction force in the tangential direction $\boldsymbol{F}_c^t$, and described as:

$$\boldsymbol{F}_c = \boldsymbol{F}_c^n + \boldsymbol{F}_c^t , \tag{25}$$

where the superscript n and t represent normal and tangential direction. The each force $\boldsymbol{F}_c^n$ and $\boldsymbol{F}_c^t$ is written as:

$$\boldsymbol{F}_c^n = (-k\delta^n - \eta |\boldsymbol{v}_r^n|)\boldsymbol{n} , \tag{26}$$

$$\boldsymbol{F}_c^t = \begin{cases} (-k\delta^n - \eta |\boldsymbol{v}_r^t|)\boldsymbol{t} & |\boldsymbol{F}_c^t| < \mu |\boldsymbol{F}_c^n| \\ -\mu |\boldsymbol{F}_c^n| \boldsymbol{t} & |\boldsymbol{F}_c^t| \geq \mu |\boldsymbol{F}_c^n| \end{cases}, \tag{27}$$

where k, δ, η, $\boldsymbol{n}$ and $\boldsymbol{t}$ are the stiffness, the displacement, the damping coefficient, normal and tangential unit vector. The damping coefficient η is given by

$$\eta = -2\ln(e) \sqrt{\frac{k}{\ln^2(e) + \pi^2} \frac{2m_i m_j}{m_i + m_j}} , \tag{28}$$

where e is the coefficient of restitution. The torque is calculated from the tangential contact force.

$$\sum \boldsymbol{T} = \sum \boldsymbol{l} \times \boldsymbol{F}_c^t , \tag{29}$$

where $\boldsymbol{l}$ indicates the vector from the center of a particle to a contact point.

The drag force $\boldsymbol{F}_d$ has the same meaning as the interaction force. Therefore, the resistance force for fluid is adopted to the drag force for soil. The drag force acting on one particle is given by:

$$\boldsymbol{F}_d = \begin{cases} a(\varepsilon)\varepsilon\boldsymbol{v}_r + b(\varepsilon)\varepsilon^2\boldsymbol{v}_r|\boldsymbol{v}_r|\frac{V_s}{1-\varepsilon} & (\varepsilon < 0.8) \\ \frac{3}{4}C_d\frac{(1-\varepsilon)\rho_f\boldsymbol{v}_r|\boldsymbol{v}_r|}{d_s}\varepsilon^{-2.7}\frac{V_s}{1-\varepsilon} & (\varepsilon \geq 0.8) \end{cases}, \tag{30}$$

where d_s means the diameter of a soil particle.

4 ANALYSIS

4.1 Validation test

As a validation test, water and glass beads dam break flow analysis is implemented. This is already experimented by Xiaosong Sun et al. [4], and the analysis is validated by comparing with the experimental result. In this experiment, the glass beads are sphere. The dimension of the tank is shown in Fig 3, and the water and glass beads are steady in the tank initially. At time t = 0, the gate is pulled up in a vertical direction with 0.68m/s and the water and glass beads start to move. The computational parameters are shown in Table. 1. Time increment in this analysis is 0.0001s.

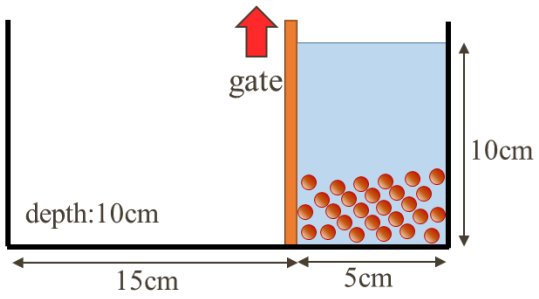

Figure 3: Analysis model of the dam break test

Table 1: Computational parameters

Fluid phase			
Particle number	Initial particle distance (cm)	Density (g/cm^3)	
13943	0.3	1.0	
Solid phase			
Particle number	Particle diameter (cm)	Density (g/cm^3)	Restitution coefficient
7920	0.3	2.5	0.9
Stiffness (N/m)		Friction coefficient	
1000		0.2	

As a qualitative comparison, the snapshots of analytical and experimental result are shown in Fig 4 for the instants of $t = 0.05$, 0.1, 0.15 and 0.2 sec. The analytical results show good agreement with the experiment.

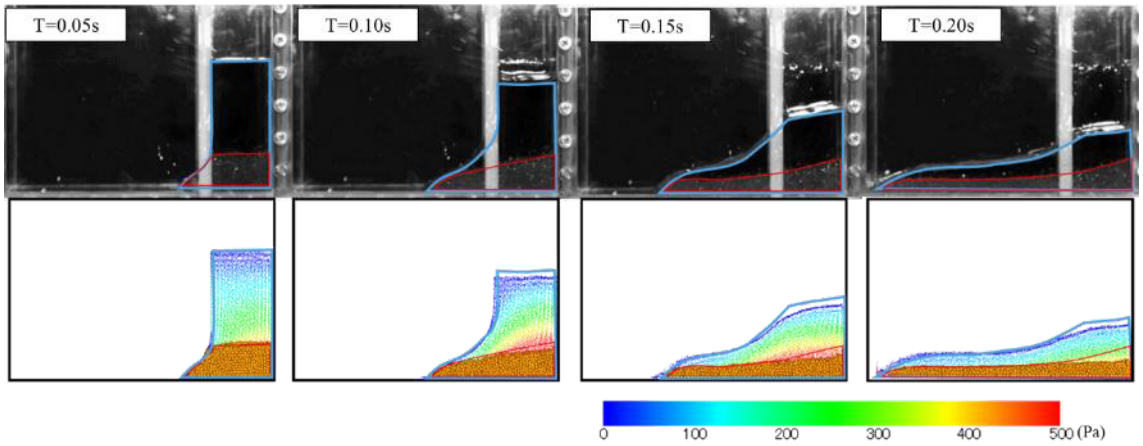

Figure 4: Comparison between experimental and analytical results
Blue and red lines highlights the water and glass beads domain respectively

As a quantitative comparison, the front position data of water and glass beads of the experiment measured by Xiaosong Sun et al. are compared with the analysis. The dimensionless number z^* and t^* are defined as by the tank size $a = 5cm$:

$$t^* = \mathrm{t}\sqrt{\frac{2g}{a}}, \tag{31}$$

$$z^* = \frac{z}{a}, \tag{32}$$

where z is the front positions of water and glass beads. The normalized positon of water and glass beads are plotted in Fig 5, the match between experiment and analysis for water and glass beads can be seen from it.

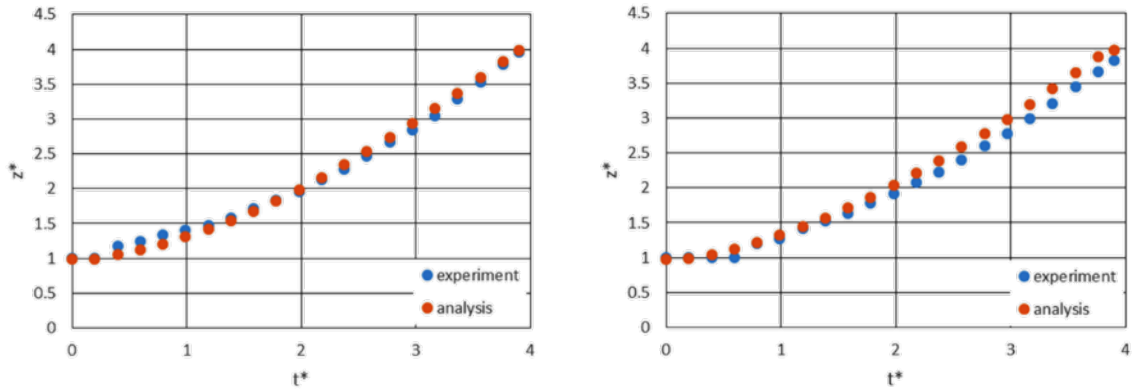

Figure 5: Comparison by the front position of water and glass beads

5 SCOURING AND PIPING ANALYSIS

The proposed SPH-DEM coupled method are validated by the dam break flow test. In this section, this method is applied to the scouring and seepage-induced piping analysis. In this

analysis, only the destruction of the mound is considered.

5.1 Validation test

In general, the breakwater mound is composed of soils, which moves individually. After the mound scouring is judged by our simulation result with the SPH method in the fluid domain, each soil's motion can be modeled by the DEM. However, the direct representation of the soil motion by the DEM induces high computational cost simulation in general. In this study, a macroscopic scouring and piping criterion are utilized to reduce the cost. The scouring and seepage-induced piping occur on the surface of the mound. Therefore, all the DEM particle is fixed in the original position, and only the surface soil DEM particle will be judged by the macroscopic empirical criterion. After the judgement of scouring and/or piping, the DEM soil particle will be moved by DEM manner. In this method, the number of analyzed DEM is much small and the cost is also lower. In addition, it is possible to distinguish whether the soil moves by the scouring of piping.

The criterion of the scouring is composed of active force F_a which moves the surface soil and resistance force F_r which is derived from friction force, if the active force is greater than the resistance force, the soil is judged as scoured.

$$F_a = \{\boldsymbol{F}_d + (\rho_s V_s \boldsymbol{g}) + \boldsymbol{F}_b\} \cdot \boldsymbol{t}, \tag{33}$$

$$F_r = \mu\{\boldsymbol{F}_d + (\rho_s V_s \boldsymbol{g}) + \boldsymbol{F}_b\} \cdot \boldsymbol{n}, \tag{34}$$

$$|F_a| > |F_r|. \tag{35}$$

The seepage-induced piping occurs when the hydraulic gradient defined as the gradient of the piezo water head excesses the critical hydraulic gradient. The hydraulic gradient $\boldsymbol{I}$ and the critical hydraulic gradient I_c can be calculated as follows:

$$\boldsymbol{I} = \frac{\nabla P}{\rho_f \boldsymbol{g}} + \nabla z, \tag{36}$$

$$I_c = \frac{G_s - 1}{1 + e}, \tag{37}$$

where z is the height from the arbitrary datum. G_s and e defined as $G_s = \rho_s/\rho_f$ and $e = \varepsilon/1 - \varepsilon$ respectively. However, the dimension of the hydraulic gradient and the critical hydraulic gradient are different. Therefore, the norm of the hydraulic gradient is utilized to compare these gradient. The criterion of the seepage-induced piping is given by:

$$|\boldsymbol{I}| > I_c. \tag{38}$$

However, this criterion can be applied to only a horizontal mound. The mound of the breakwater has the horizontal place but also the sloping place. Thus, the criterion of the piping is modified as:

$$|\boldsymbol{I}| > I_c n_y, \tag{39}$$

where n_y is the unit vector perpendicular to the slope.

5.2 Scouring and piping test

The analysis of the soil scouring and piping of the breakwater is done as a basic study. Here, the scouring and piping is analyzed individually.

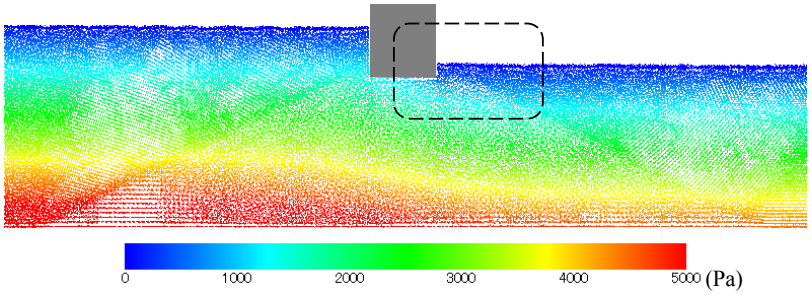

(a) Analysis result of water

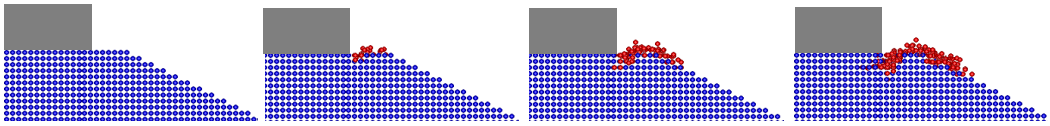

(b) Analysis result of soil
Judged particles are coloered red

Figure 6: The piping analysis result

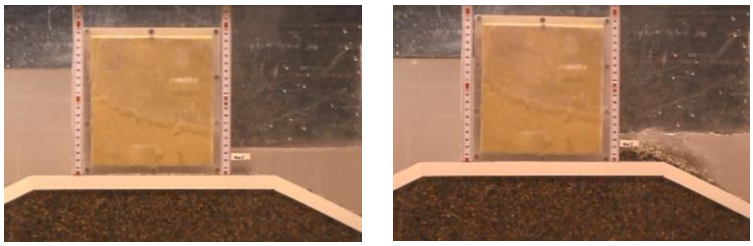

(a) Initial state (b) Piping occured

Figure 7: Snapshots of the piping experiment

At first, the piping analysis is shown in Fig 6. In this analysis, the seepage flow in the mound of breakwater occurs because of the water-level difference between the inside and outside of the port. From the soils' motion observed, this phenomena is similar to the experiment shown as Fig 7.

Next, the scouring analysis is shown in Fig 8 In this analysis, the soils are scoured along the flow.

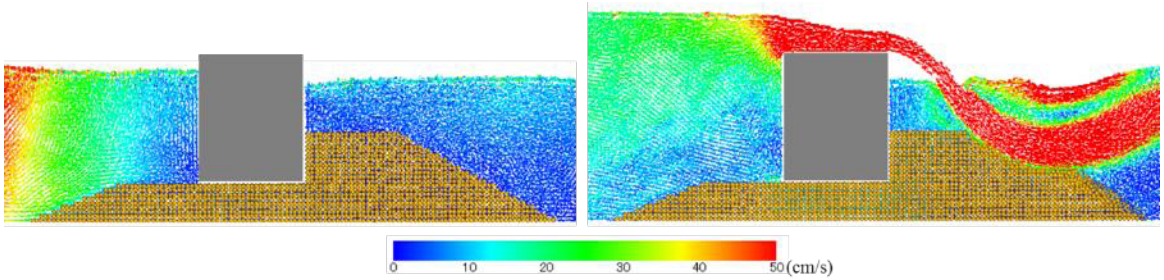

(a) Initial state (b) Piping occured

Figure 8: Analysis result of scouring

6 CONCLUSIONS

In this study, a SPH-DEM coupled method for the fluid-soil multiphase flow is developed to simulate the scouring and seepage-induced piping of breakwater. The interaction force between fluid and solid is considered to couple the SPH method for the fluid analysis and DEM for solid analysis, the unified governing equation including the interaction force based on Akbari and Wen and Yu is adopted for the fluid. For solid analysis, the interaction force is considered as the drag force. The water and glass beads dam break flow is analyzed to validate this method, and it shows a good agreement with experimental data. For scouring and seepage-induced piping, the criterion to estimate them is proposed. A good tendency is given from simple scouring and piping analysis. As the future works, a validation test will be conducted with experiment, finally this method would be expanded to simulate the collapse of a breakwater by Tsunami.

REFERENCES

[1] M. Asai, Aly, AM., Y. Sonoda and Y. Sakai, A stabilized incompressible SPH method by relaxing the density invariance condition, *Int. J. for Applied Mathematics*, Vol. 2012, Article ID 139583, 2012.

[2] Akbari, H., Modified moving particle method for modeling wave interaction with multi layered porous structures, *Coast. Eng*., Vol.89, pp.1-19, 2014.

[3] C. Wen. and Y. Yu., Mechanics of fluidization, *Chemical Engineering Progress Symposium Series 62*, 100, 1966.

[4] Xiaosong Sun, Mikio Sakai and Yoshinori Yamada, Three-dimensional simulation of a solid-liquid flow by the DEM-SPH method, *Journal of Computational Physics,* Vol.248, p.147-176, 2013.